ELSEVIER

Environmental Pollution 120 (2002) 415–422

ENVIRONMENTAL POLLUTION

www.elsevier.com/locate/envpol

Photocatalytic oxidation of NO_x gases using TiO_2: a surface spectroscopic approach

J.S. Dalton, P.A. Janes, N.G. Jones, J.A. Nicholson, K.R. Hallam, G.C. Allen*

Interface Analysis Centre, University of Bristol, Oldbury House, 121 St. Michael's Hill, Bristol BS2 8BS, UK

Received 11 June 2001; accepted 31 December 2001

"Capsule": *X-ray photoelectron spectroscopy (XPS) and Raman spectroscopy were used to study surface reactions between nitrogen oxides and TiO_2 on surfaces.*

Abstract

The bandgap of solid-state TiO_2 (3.2 eV) enables it to be a useful photocatalyst in the ultraviolet ($\lambda < 380$ nm) region of the spectrum. A clean TiO_2 surface in the presence of sunlight therefore enables the removal of harmful NO_x gases from the atmosphere by oxidation to nitrates. These properties, in addition to the whiteness, relative cheapness and non-toxicity, make TiO_2 ideal for the many de-NOX catalysts that are currently being commercially exploited both in the UK and Japan for concrete paving materials in inner cities.

There is need, however, for further academic understanding of the surface reactions involved. Hence, we have used surface specific techniques, including X-ray photoelectron spectroscopy and Raman spectroscopy, to investigate the NO_x adsorbate reaction at the TiO_2 substrate surface.

Keywords: Titanium dioxide; Nitrogen oxides; Photocatalyst; Raman spectroscopy; X-ray photoelectron spectroscopy

1. Introduction

Due to the increase in harmful emission gases in the World's inner cities, it is apparent that there is a need to remove pollutants, such as nitrogen oxides, NO_x, and sulphur dioxide, SO_2, from the atmosphere. Not only do these gases pose a threat to health, they are also causing degradation to many inner city buildings (Allen et al., 2000). Despite attempts to lower these emissions from cars, it appears that a way of removing such pollutants once in the atmosphere needs to be sought. Inorganic photocatalysts, such as titanium dioxide, have very recently been exploited and shown to be a relatively cheap and effective way of removing organic poison compounds and pollutant gases from both air and aqueous environments (Bilmes et al., 2000; Chen et al., 1997; Hashimoto et al., 2000; Nakamura et al., 2000; Ohtani et al., 1997; Wu et al., 2000). This paper concentrates on using TiO_2 as a photocatalyst for removing NO_x gases from the atmosphere.

Titanium dioxide is a semiconductor photocatalyst with a band gap of energy 3.2 eV. The band structure of TiO_2 is discussed more fully elsewhere (Daude et al., 1977). When subjected to ultraviolet photon radiation of wavelength less than 380 nm, a valence band electron is promoted to the conduction band, creating an electron-hole pair that can participate in various oxidation-reduction chemical reactions. Here, it is shown that the harmful NO_x gases are oxidised to nitrates by utilising UV radiation to activate the TiO_2. These nitrates are easily consumed and recycled by plants. It has been shown that the photocatalytic effect of TiO_2 is dependent on crystal structure, particle size and surface area and that the effectiveness of the process is governed by the lifetime, or recombination probability, of the electron-hole pair (Bilmes et al., 2000; Hashimoto et al., 2000; Nakamura et al., 2000).

In this paper, X-ray photoelectron spectroscopy (XPS) and Raman spectroscopy are used to study the surface reaction between the nitrogen oxides and the TiO_2 surface. XPS can give information on molecular chemical environments and atomic quantitative analysis in the top 5 nm of the surface. It is the ideal technique

* Corresponding author. Fax: +44-117-925-5666.
E-mail address: g.c.allen@bristol.ac.uk (G.C. Allen).

0269-7491/02/$ - see front matter
PII: S0269-7491(02)00107-0

for differentiating adsorbed nitrogen species, such as NH_3, NO, NO_2 and NO_3^-, and it is shown that the amount of converted nitrate on the surface can be monitored quantitatively by XPS. Raman spectroscopy gives information on both the crystal structure of the substrate and bonding characteristics of adsorbed atoms and molecules.

2. Materials and methods

2.1. Materials

Two samples of titanium dioxide were studied. One was an unknown commercial sample and the other obtained from May and Baker laboratory chemicals (purity > 98%). The NO_x gas used was from Air Products and certified as 109 ± 5 ppm in $21.0 \pm 0.4\%$ oxygen, balance nitrogen. The mixer gas used to dilute the NO_x concentration given above was dry air (Air Products).

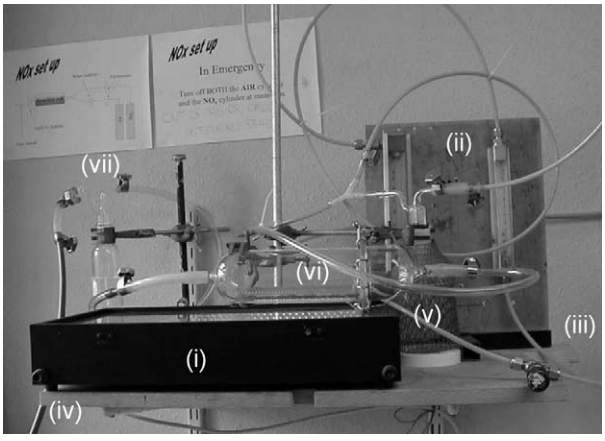

Fig. 1. Apparatus for NO_x gas removal. Shown are: (i) UV exposure box; (ii) gas flow meters; (iii) NO_x gas and air mixer gas in; (iv) gas out; (v) water bubbler for air mixer gas; (vi) glass reaction vessel; and (vii) sodium hydroxide bubbler for excess NO_x removal.

The UV exposure unit consisted of 4×60 W strip tubes and was manufactured by Radio Spares, model No. 556-238. The reaction vessel was made from glass of approximate thickness 3 mm, which allowed > 80% transmission of radiation at $\lambda = 320$ nm.

The gas flow and reaction vessel set-up was constructed in-house and is shown in Fig. 1. The system was constructed with flow meters to allow an NO_x concentration of between 10 and 100 ppm when used in conjunction with the air mixer gas. A water bubbler allowed the reaction to be studied with wet or dry gas while a second bubbler, containing aqueous sodium hydroxide solution, was used after the reaction vessel to remove any unreacted NO_x.

2.2. Methods

2.2.1. Scanning electron microscopy (SEM)

The SEM used was a commercial Hitachi S2300 instrument with a tungsten hairpin filament. An accelerating voltage of 25 keV was used and samples were gold coated to eliminate charging.

2.2.2. X-ray photoelectron spectroscopy (XPS)

XPS analyses the near-surface of materials with analysis depths up to 5 nm. It can provide quantitative chemical information as well as oxidation and structural environments on all elements apart from hydrogen and helium. Soft X-rays, of energy hν, excite electrons from valence and core orbitals of surface atoms, as shown in Fig. 2. The kinetic energy of the ejected electron, E_K, is measured by an electron energy analyser. These photoelectrons have energies according to the relationship (Briggs and Seah, 1992):

$$E_B = h\nu - E_K - \Phi$$

where Φ is the work function of the spectrometer. E_B is the binding energy of the photoelectron to the parent

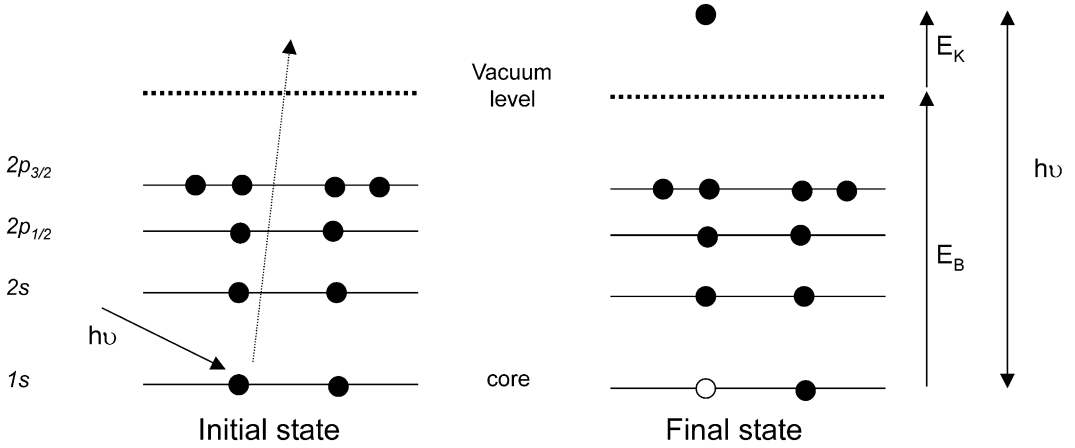

Fig. 2. Schematic showing XPS process. E_B is the electron binding energy and E_K is the electron kinetic energy.

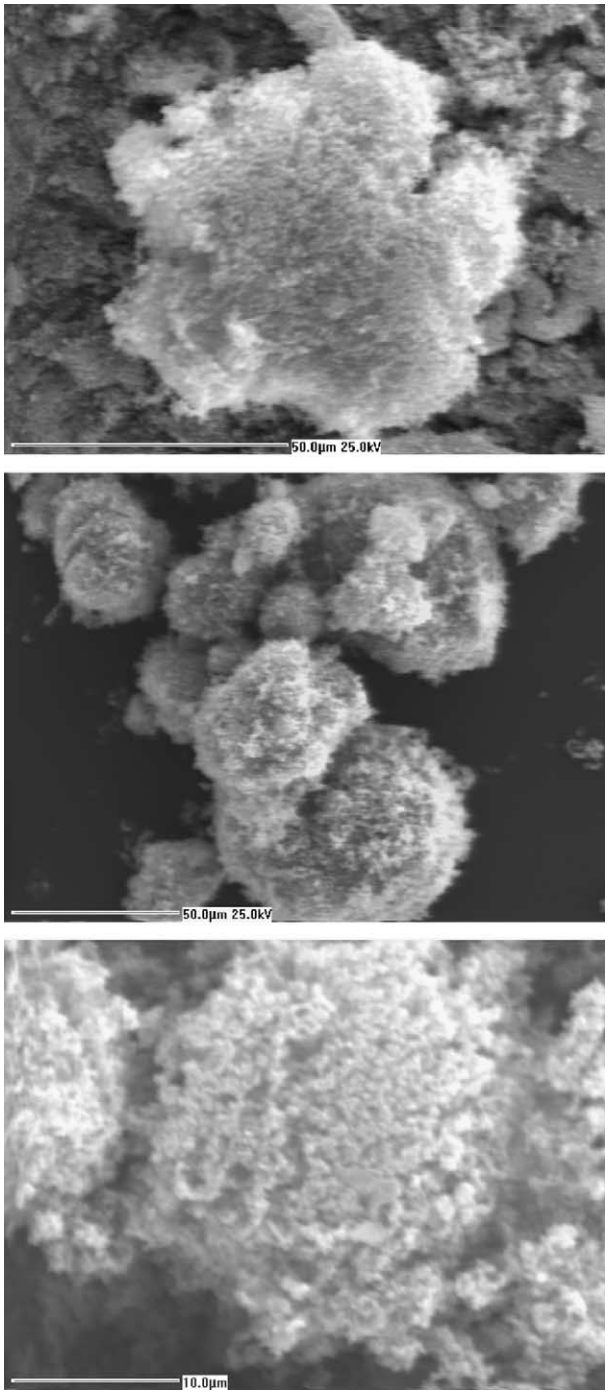

Fig. 3. SEM images of TiO_2 particles on silica support.

atom and can be calculated from the other measured and known values. XPS spectra are traditionally plotted as photoelectron signal intensity against E_B. XPS peaks can then be identified using tabulated binding energy values from XPS handbooks yielding information on chemical composition and bonding environments (Moulder et al., 1992).

XPS spectra were acquired using a VG Scientific Escascope spectrometer using Mg K_α X-rays (300 W; 15 kV, 20 mA) and a hemispherical electron energy analyser. Data acquisition and manipulation were carried out using manufacturer-supplied VGS5250 software. During acquisition of spectra, the pressure in the main chamber was maintained at $\sim 8\times10^{-9}$ Torr to ensure a clean sample surface. Charge referencing was carried out against adventitious hydrocarbon (C *1s* = 284.8 eV) (Moulder et al., 1992, p. 22) from pump oil contamination.

Table 1
Quantitative surface atomic percentage XPS analyses on NO_x-treated and control UV-activated TiO_2 samples

	Control	NO_x exposure
C *1s*	41.5±5	38.6±5
O *1s*	45.4±5	46.5±5
Ti *2p*	12.7±2	13.3±2
N *1s*		
as organic	0.6±0.2	0.6±0.2
as NO_3^-	0.0	0.7±0.2

Error bars are calculated from at least five repeat measurements.

2.2.3. Raman spectroscopy

In Raman spectroscopy, a laser is directed at the sample. The majority of the light is elastically scattered (Rayleigh light). However, a small fraction is scattered inelastically and the energy difference between the incident and reflected beam, often measured in wavenumber, cm^{-1}, corresponds to a change in molecular vibration within the sample. These characteristic bond vibrations allow chemical and crystal state identification of the sample.

Raman spectra were acquired on a Renishaw System 2000 imaging Raman microscope using a 20 mW helium–neon (He–Ne) laser with an emission wavelength of 632.8 nm. The scan range was set to monitor between 0 and 3000 cm^{-1} with the analyser removing any effects of cosmic rays. The He–Ne laser analyses up to a few micrometers into the surface.

3. Results

3.1. Scanning electron microscopy

SEM images of a colloidal suspension of TiO_2 dried and deposited onto silica are shown in Fig. 3. These show the average size of the particles was less than 1 µm. These sub-micron TiO_2 particles with large surface area are most ideal for this study.

3.2. Raman spectroscopy

Although Raman spectroscopy has been extensively used to study TiO_2 (Felske and Plieth, 1989), it is

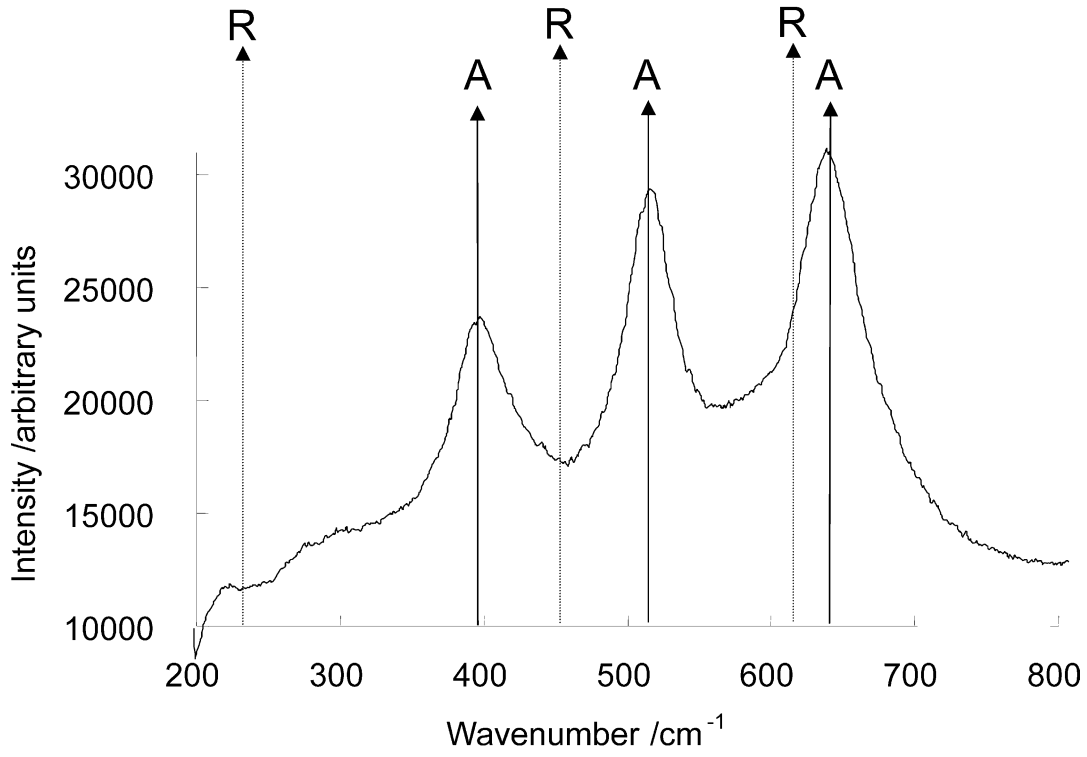

Fig. 4. Raman spectrum of TiO_2 sample showing anatase crystal structure. 'A' corresponds to a band or vibrational mode for anatase and 'R' corresponds to rutile. For reference see text.

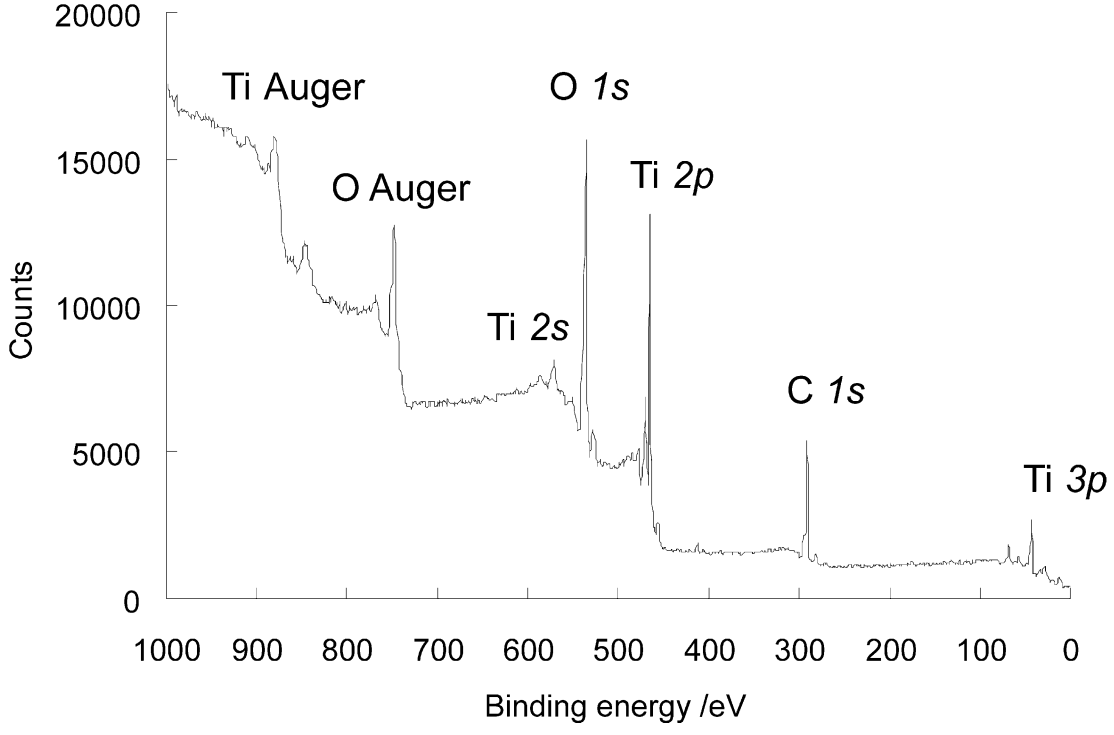

Fig. 5. Typical XPS spectrum of TiO_2 powder.

worthwhile including this technique here as it is a rapid way of obtaining the surface crystal structure of the TiO_2, which is believed to be important in the efficacy of the NO_x removal (Ohtani et al., 1997). The Raman spectrum of the TiO_2 powder used here is shown in Fig. 4, with the characteristic bands giving evidence for the crystalline form of anatase rather than rutile or brookite (Felske and Plieth, 1989). A highly crystalline

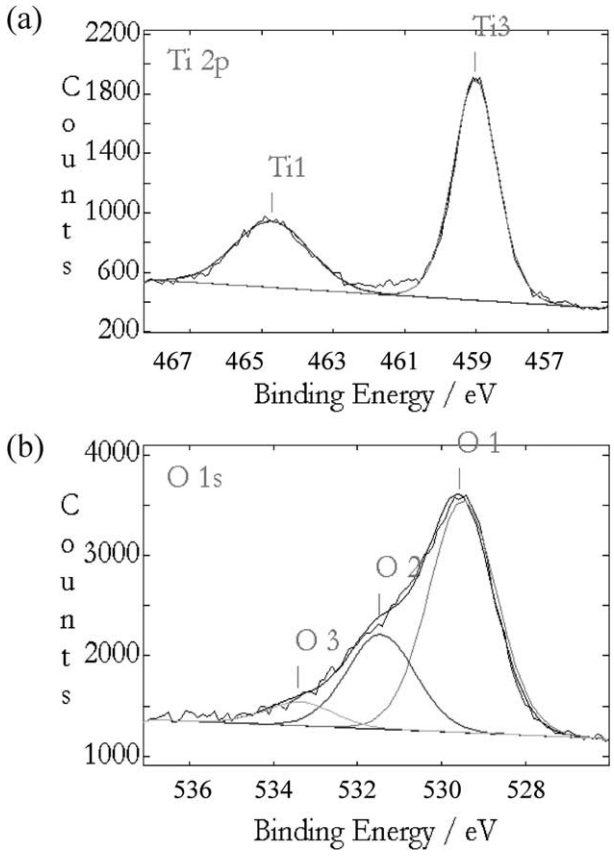

Fig. 6. (a) Regional XPS scan for Ti *2p*. (b) Regional XPS scan for O *1s*.

anatase surface with fewer defects is thought to increase the electron-hole lifetime of the TiO_2 after UV photon irradiation (Ohtani et al., 1997). Amorphous TiO_2 contains imperfections in the crystal surface, such as ionic impurities and dangling bonds. These can cause other electronic states to be present in the bandgap, shortening the recombination probability. Ionic impurities in the surface of TiO_2 can be detected by XPS.

3.3. X-ray photoelectron spectroscopy

A typical wide scan XPS survey spectrum of the untreated commercial TiO_2 powder is shown in Fig. 5. Distinct photoelectron peaks are seen for various oxygen and titanium electron orbitals on the characteristic stepwise background. Auger peaks (Briggs and Seah, 1992) are also observed. A C *1s* peak is observed due to deposition of adventitious hydrocarbon on the sample's surface from the oil diffusion pumps evacuating the analysis chamber (Briggs and Seah, 1992). Fig. 6 shows typical regional scans of the: (a) Ti *2p*; and (b) O *1s* peaks. Spin-orbit coupling of the Ti *2p* peak gives rise to the two components $2p_{3/2}$ and $2p_{1/2}$. Fitting the Ti *2p* peaks to Gaussian–Lorentzian curves showed only one oxidation state of Ti. The fit to the O *1s* peak indicated three components characteristic of TiO_2, Ti–OH and

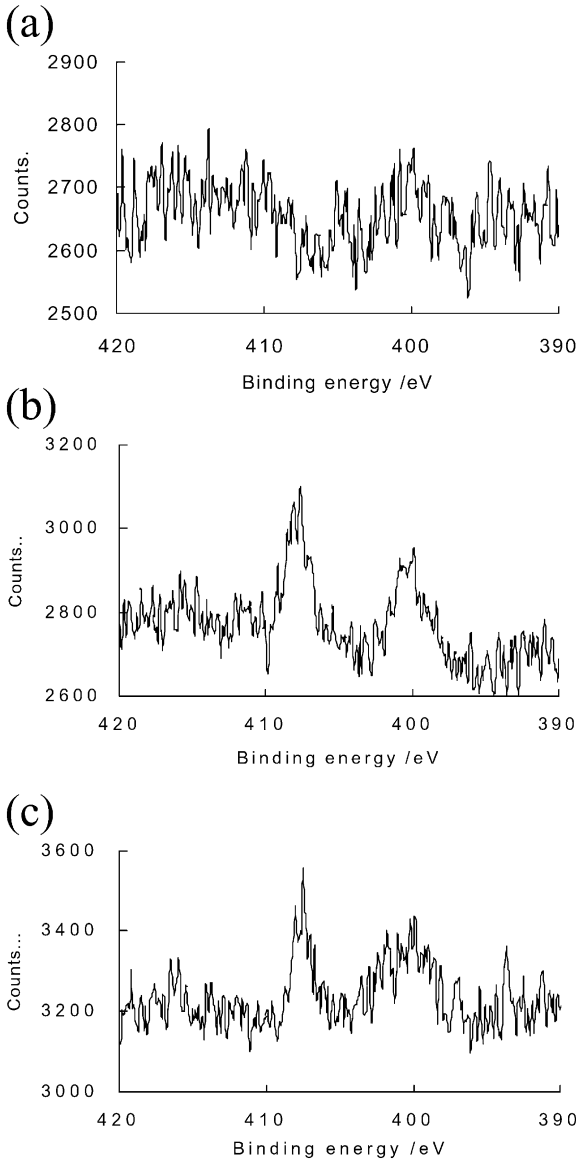

Fig. 7. Regional XPS scans for N *1s*: (a) typical spectrum for control experiment when TiO_2 not subjected to UV radiation; (b) typical spectrum for the commercial TiO_2 sample when subjected to NO_x gases and UV radiation; and (c) typical spectrum for the May and Baker TiO_2 sample when subjected to NO_x gases and UV radiation.

Ti–OH_2, successively with increasing binding energy (Moulder et al., 1992, pp. 44–45, 230–232). Titanium hydroxide species are often formed at the very surface due to broken and dangling bonds from the oxygen that have to be terminated. In addition, a small amount of bound surface water is often detected, even in ultrahigh vacuum conditions. It has been suggested that these surface hydroxyls contribute to the NO_x removal process (Ohtani et al., 1987; Oosawa and Graetzel, 1988).

TiO_2 samples were subjected to NO_x at a concentration range from 10 to 100 ppm and UV exposure of between 6 and 48 h. It was observed that the formation of reaction products did not vary significantly with either exposure time or NO_x concentration. Fig. 7(a)

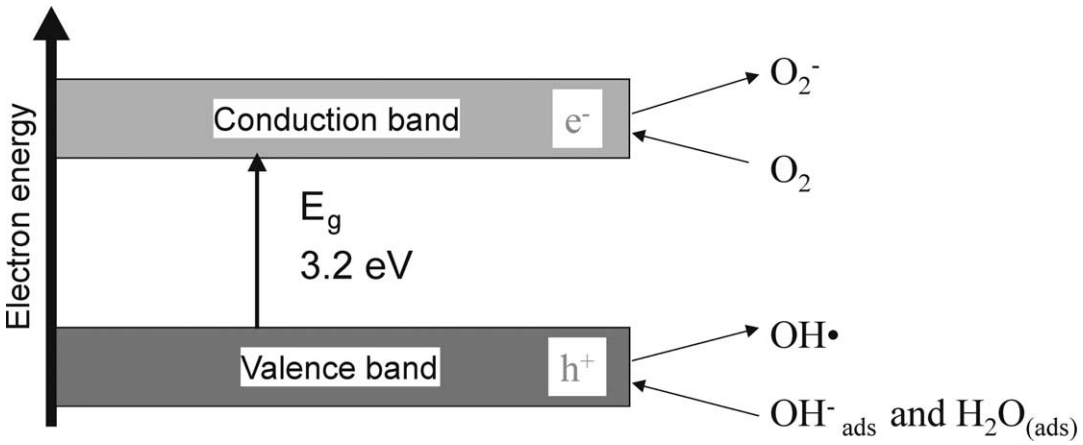

Fig. 8. Suggested mechanisms for photocatalytic reaction of TiO_2 at the valence and conduction band.

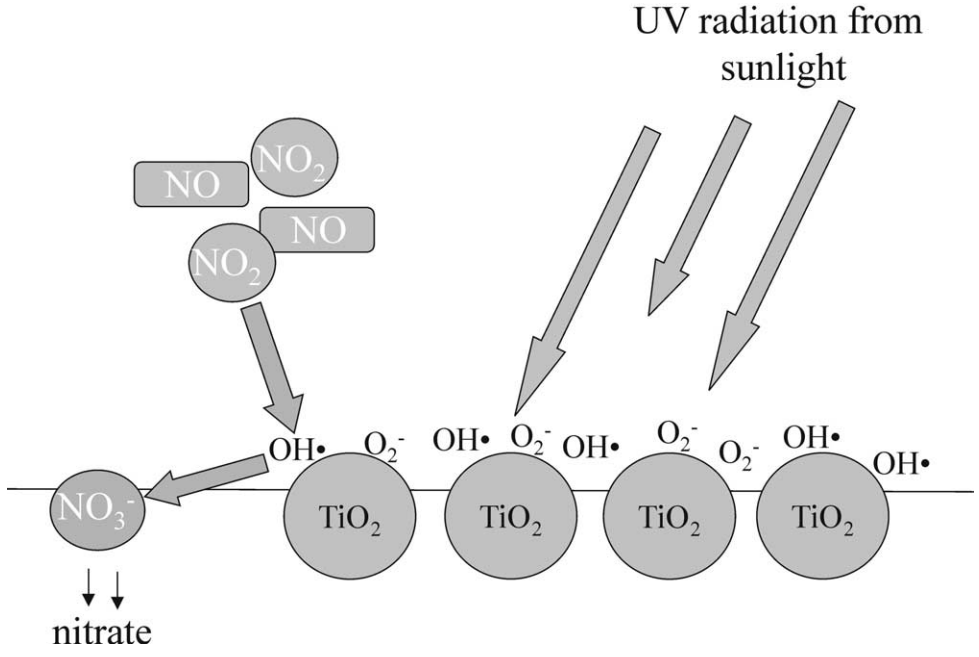

Fig. 9. Schematic showing NO_x removal process.

shows a typical control experiment scan whereby the TiO_2 was exposed to moist NO_x but not to UV light. Fig. 7(b, c) show UV and moist NO_x exposure to the commercial sample and May & Baker sample, respectively. Multiple experiments of this kind showed reproducible peaks at 400.0 ± 0.3 and 408.2 ± 0.3 eV after charge correction. The peak at 400.0 eV is due to organic nitrogen, which may be an impurity on the surface of the TiO_2. Manufacturers often pre-adsorb ammonium salt surfactants on the surface of TiO_2 at low concentrations to act as dispersing agents, in order to create stable colloidal solutions. It can be seen that in Fig. 7(c) this peak is quite broad. This was also sometimes observed for the commercial sample. This could be due to either various organic nitrogen moeities or salts being present on the surface or to unreacted NO left adsorbed on the surface (Allen et al., 2000). The peak at 408.2 eV is characteristic of nitrates (Briggs and Seah, 1992; Moulder et al., 1992, p. 43), the reaction product of the nitrogen oxide gases with photoactive TiO_2. XPS is a quantitative surface technique and the atomic percentage compositions of the top 5 nm of the surfaces are shown in Table 1. Error values were obtained from multiple measurements. The C *1s* atomic percentage was kept to a minimum by washing the TiO_2 in water before study, which appeared effective in removing lower mass hydrocarbons. The amount of N *1s* present on the surface was not significant enough to have an affect on either the Ti *2p* or O *1s* peaks.

The schematic in Fig. 8 shows the redox processes occurring at the active TiO_2 sites most widely postulated in the literature. Hashimoto et al. (2000) presented

results showing that UV irradiation of TiO_2 in the presence of oxygen gave O_2^- with the free radical in the TiO_2. These superoxide ions then reacted with nitrogen oxides to form nitrates (Hashimoto et al., 2000). Given the results obtained in this paper, a suggested stepwise mechanism is given in Reaction Scheme 1. It is proposed that the surface hydroxyls increase efficacy of the process and participate by reacting with three molecules of NO_2 leaving two molecules of nitrate and one molecule NO, which can be removed by process 2(a) or 2(b).

4. Discussion

Experiments carried out here have shown that TiO_2 is effective at converting nitrogen oxides to harmless nitrates and how XPS can be used to quantify the efficiency of the reaction. The schematic in Fig. 9 summarises the reaction. It is apparent from the literature that highly crystalline anatase is the most photoactive form of titania and Raman spectroscopy is a quick and simple way of ascertaining surface crystal structure. XPS can detect ionic impurities at levels greater than 0.1% in the first 5 nm that may affect the band structure. Due to its surface sensitivity and ability to determine chemical environment, XPS is also ideal for analysing adsorbed species resulting from processes such as those described here.

5. Conclusions

1. TiO_2 is effective at converting nitrogen oxides to harmless nitrates and XPS can be used to quantify the efficiency of the reaction while Raman spectroscopy is a quick and simple way of ascertaining surface crystal structure.
2. Only one oxidation state of Ti was observed on the untreated TiO_2 materials but the O *1s* peak indicated three components characteristic of TiO_2, Ti–OH and Ti–OH_2.

(1) Photocatalysis

$$TiO_2 + h\upsilon \longrightarrow TiO_2^* (h^+_{vb} + e^-_{cb}) \quad \text{charge carrier generation}$$

$$OH^-_{(ads)} + h^+_{vb} \longrightarrow OH\bullet_{(ads)} \quad \text{hole trapping}$$
$$O_{2\,(ads)} + e^-_{cb} \longrightarrow O_2^-{}_{(ads)} \quad \text{electron trapping}$$

(2a) Oxidation using hydroxyl radicals: OH•

$$\text{(a) } NO_{(g)} + 2OH\bullet_{(ads)} \longrightarrow NO_{2\,(ads)} + H_2O_{(ads)}$$
$$\text{or (b) } NO_{2\,(ads,g)} + OH\bullet_{(ads)} \longrightarrow NO_3^-{}_{(ads)} + H^+_{(ads)}$$

(2b) Oxidation using "active oxygen": O_2^-

$$NO_{x\,(ads)} \xrightarrow{O_2^-{}_{(ads)}} NO_3^-{}_{(ads)}$$

(2c) Reaction with Ti-OH via disproportion[3]

$$3NO_2 + 2OH^- \longrightarrow 2NO_3^- + NO + H_2O$$

(3) Removal of [HNO_3] complex from surface of block by water

$$[HNO_3]_{(ads\ on\ block)} \longrightarrow HNO_{3\,(aq)}$$

Reaction Scheme 1.

3. The reaction products observed were independent of the time of exposure or NO_x concentration.
4. After exposure, nitrogen peaks attributable to organic species (also present before reaction) and possibly unreacted NO adsorbed on the surface were seen, together with nitrate anions.
5. Given the results obtained in this paper, a suggested stepwise mechanism is presented. It is proposed that the presence of hydroxyl groups on the surface increases the efficacy of the process.

Acknowledgements

The authors would like to thank Paul Livesey and Stuart Pepper from Castle Cement for interesting discussions and advice on this work. Gareth Hughes is thanked for carrying out the Raman measurements.

References

Allen, G.C., El-Turki, A., Hallam, K.R., McLaughlin, D., Stacey, M., 2000. Role of NO_2 and SO_2 in degradation of limestone. British Corrosion Journal 35, 35–48.

Bilmes, S.A., Mandelbaum, P., Alvarez, F., Victoria, N.M., 2000. Surface and electronic structure of titanium dioxide photocatalysts. J. Phys. Chem. B. 104, 9851–9858.

Briggs, D., Seah, M.P. (Eds.), 1992. Practical Surface Analysis, second ed., vol. 1. John Wiley, Chichester.

Chen, L.X., Rajh, T., Wang, Z., Thurnauer, M.C., 1997. XAFS studies of surface structures of TiO_2 nanoparticles and photocatalytic reduction of metal ions. J. Phys. Chem. B. 101, 10688–10697.

Daude, N., Gout, C., Jouanin, C., 1977. Electronic band structure of titanium dioxide. Physical Review B 15, 3229–3235.

Felske, A., Plieth, W.J., 1989. Raman spectroscopy of titanium dioxide layers. Electrochimica Acta 34, 75–77.

Hashimoto, K., Wasada, K., Toukai, N., Kominami, H., Kera, Y., 2000. Photocatalytic oxidation of nitrogen monoxide over titanium (VI) oxide nanocrystals large size areas. J. Photochem and Photobiol. A: Chemistry 136, 103–109.

Moulder, J.F., Stickle, W.F., Sobol, P.E., Bomben, K.D., 1992. In: Chastain, J. (Eds.), Handbook of X-ray Photoelectron Spectroscopy. Perkin-Elmer Corporation, Minnesota.

Nakamura, I., Negishi, N., Kutsuna, S., Ihara, T., Sugihara, S., Takeuchi, K., 2000. Role of oxygen vacancy in the plasma treated TiO_2 photocatalyst with visible light activity for NO removal. J. Molecular Catalysis A: Chemical 161, 205–212.

Ohtani, B., Okugawa, Y., Nishimoto, S., Kagiya, T., 1987. Photocatalytic activity of TiO_2 powders suspended in aqueous silver nitrate solution—correlation with pH dependent surface structures. J. Phys. Chem. 91, 3550–3555.

Ohtani, B., Ogawa, Y., Nishimoto, S., 1997. Photocatalytic activity of amorphous-anatase mixture of titanium (VI) oxide particles suspended in aqueous solutions. J. Phys. Chem. B 101, 3746–3752.

Oosawa, Y., Graetzel, M., 1988. Effect of surface hydroxyl density on photocatalytic oxygen generation in aqueous TiO_2 suspensions. J. Chem. Soc. Faraday Trans 1, 84. 197-205.

Wu, W.-C., Chuang, C.-C., Lin, J.-L., 2000. Bonding geometry and reactivity of methoxy and ethoxy groups adsorbed on powdered TiO_2. J. Phys. Chem. B 104, 8719–8724.